Journal of Medicinal Chemistry

Article

Structure-Activity-Relationships of Benzimidazole-based Glutaminyl Cyclase Inhibitors Featuring a Heteroaryl-scaffold

Daniel Ramsbeck, Mirko Buchholz, Birgit Koch, Livia Böhme, Torsten Hoffmann, Hans-Ulrich Demuth, and Ulrich Heiser

J. Med. Chem., **Just Accepted Manuscript** • DOI: 10.1021/jm4001709 • Publication Date (Web): 25 Jul 2013

Journal of Medicinal Chemistry is published by the American Chemical Society. 1155 Sixteenth Street N.W., Washington, DC 20036

Structure-Activity-Relationships of Benzimidazole-based Glutaminyl Cyclase Inhibitors Featuring a Heteroaryl-scaffold

Daniel Ramsbeck[†§], *Mirko Buchholz*[†], *Birgit Koch*[‡], *Livia Böhme*[∞], *Torsten Hoffmann*[∞], *Hans-Ulrich Demuth*[†,‡,∞] *and Ulrich Heiser*[*,†].

[†]Department of Medicinal Chemistry,

[‡]Department of Enzymology

[∞]Department of Preclinical Pharmacology,

Probiodrug AG, Weinbergweg 22, 06120 Halle, Germany.

[§]present address: Fraunhofer Institute for Cell Therapy and Immunology, Perlickstraße 1, 04103 Leipzig, Germany

RECEIVED DATE

ABSTRACT. Glutaminyl cyclase (hQC) has emerged as a new potential target for the treatment of Alzheimer's Disease (AD). The inhibition of hQC prevents of the formation of the Aβ$_{3(pE)-40,42}$-species which were shown to be of elevated neurotoxicity and are likely to act as a seeding core leading to an accelerated formation of Aβ-oligomers and fibrils. This work presents a new class of inhibitors of hQC, resulting from a pharmacophore-based screen. Hit molecules were identified, containing benzimidazole as the metal binding group connected to 1,3,4-oxadiazole as the central scaffold. The subsequent optimization resulted in benzimidazolyl-1,3,4-thiadiazoles and -1,2,3-triazoles with an inhibitory potency in the nano-molar range. Further investigation into the potential binding mode of the new compound classes combined molecular docking and site directed mutagenesis studies.

KEYWORDS. Human glutaminyl cyclase, metal-binding-group, benzimidazole, ligand-based screening, pharmacophore model, site-directed mutagenesis, Alzheimer's Disease, pGlu-Aβ peptide, docking, 1,2,3-triazoles, 1,2,4-oxadiazoles, 1,3,4-oxadiazoles, 1,3,4-thiadiazoles, positional isomers.

Introduction. Post-translational protein modifications are playing a key role in the maturation of the majority of bioactive peptides. Among those, the formation of N-terminal pyroglutamate (pGlu) residues is commonly found in nature.[1-3] This modification on one hand increases the proteolytic stability or, on the other hand, contributes to the formation and stabilization of the bioactive conformation of the respective peptides and proteins. The formation of the N-terminal pGlu residue is catalyzed by human glutaminyl cyclase (hQC)[4] and its iso-enzyme (hisoQC).[5] QCs are highly abundant in secretory tissue such as secretory glands or brain tissue.[6,7] Both iso-enzymes are zinc-dependent and exhibit a high structural identity and similar substrate specificity. hQC is highly abundant in secretory vesicles and is co-secreted with its substrates, whereas hisoQC is a Golgi resident enzyme.[5]

Targeting the N-terminal modification of Glu or Gln into the respective pGlu has come into the focus of drug development for the treatment of Alzheimer's Disease (AD). pGlu-modified Aβ-peptides are discussed to be a crucial species involved in the early onset of AD.[8,9] These pGluAβ peptides exhibit an increased neurotoxicity and accelerated aggregation kinetics as compared to native Aβ–peptides, e.g. $A\beta_{(1-40)}$ or $A\beta_{(1-42)}$.[10,11] Furthermore, it was shown that $A\beta_{(pE3-42)}$ co-oligomerizes with an excess of $A\beta_{(1-42)}$ to form metastable low-n oligomers that then exhibit a different morphology and an elevated neurotoxicity as compared to oligomers formed by $A\beta_{(1-42)}$ alone. This neurotoxic effect requires the presence of the Tau-protein, showing a link between the Aβ- and Tau-pathology.[12] In vivo evidence regarding the involvement of hQC in the formation of pGluAβ and its effects on learning and memory was gained by hQC-transgenic and -knock-out mice models of AD.[13,14] Furthermore, the application of QC inhibitors successfully reduced the amount of pGluAβ in the brain of other transgenic mouse models of AD resulting in positive effects on learning and memory.[15,16]

Recently, we presented the first generation of QC inhibitors, based on imidazo-propylthiourea, which were later subsequently modified by bio-isosteric replacements and structure based approaches.[17,18] Based on these results, a pharmacophore-based filter was designed, applying a flexible alignment of known QC-inhibitors and a QC-substrate. The subsequent screen of a virtual library led to the medium potent benzimidazolyl-1,3,4-oxadiazole hit-compounds as a suitable chemo-type for further optimization. The optimization and SAR as well as a discussion of the potential binding mode in the active site are presented here.

Results and Discussion

3D Similarity Filtering. A flexible alignment of potent inhibitors identified earlier[17] and the substrate H-Gln-Phe-Ala-NH_2 resulted in a match of pharmacophoric features (Fig 1).[17] The resulting pharmacophore was then applied in a 3D-similarity filtering of a library containing 653218 pre-processed lead-like compounds[19-21] setting a smart-key constraint in the metal-binding part, considering only imidazole-related substructures. This was done in order to limit the number of hits to compounds containing imidazole or imidazole-related heterocycles. The rationale for this approach was the earlier identification of imidazole out of a screen of different heterocycles as potent metal-binder for hQC.[17] The search resulted in a number of 4878 hits corresponding to a hit rate of 0.75%. Among these hits, besides the expected imidazole-derivatives also benzimidazole-based compounds were identified in a remarkable high number (1760 molecules corresponding to 36.1% of all hits). This finding prompted us to examine the inhibitory potency of benzimidazole as a new type of metal-binding-group (MBG) in QC-inhibitors, resulting in a K_i-value of 150 µM (Fig.2), which is indeed comparable to the previously identified imidazole (K_i = 100 µM).[17] Consequently, with the goal to broaden the chemical space of possible QC-inhibitors by compounds featuring this new type of MBG, only benzimidazole-containing compounds were further considered. The next filtering step was set by the limitation of the allowed value for the topological polar surface area (TPSA) to be below 70 Å^2. This was done with respect to the potential ability of the compounds to pass the blood-brain-barrier (BBB). The application of the TPSA-filter and the commercially availability of the screening compounds reduced the number of the tested compounds to be 69. Among those, 9 compounds were found to be active ($K_{i,\ hQC}$ < 5 µM). The analysis of the chemical accessibility and possible ways for derivatization led to three oxadiazole-substituted benzimidazoles (Fig. 2), now serving as starting points for further potency optimization.

Chemistry. The synthesis of the different 1,3,4-oxadiazole-substituted derivatives (**5, 6** and **7**) was accomplished starting from benzimidazole-5(6)-carboxylic acid hydrazide (**3**) according to Scheme 1. The alkylthio-1,3,4-oxadiazole derivatives (**5a-h**) were yielded from **3** after reaction with carbondisulfide under basic conditions followed by alkylation of the resulting 3H-1,3,4-oxadiazole-2-thione (**4**) with different alkylhalides.[22] The respective aminoalkyl-substituted 1,3,4-oxadiazole derivative (**6**) resulted from **3** by acylation with benzylisothiocyanate and subsequent cyclization of the crude thiosemicarbazide by means of dicyclohexylcarbodiimide.[23] In case of the alkyl substituted 1,3,4-oxadiazole derivates (**7a** and **7e-g**), the benzimidazole carbohydrazide **3** was acylated with different acid chlorides followed by subsequent $POCl_3$ mediated cyclization of the bisacylhydrazide intermediates. The derivatives with inverse ether-, thio-ether- or sulfone-spacer (7**b-d**), as well as the alkyl substituted 1,3,4-oxadiazoles **7h-k** were accessible by direct treatment of **3** with different carboxylic acids in neat $POCl_3$.[24]

The 1,3,4-thiadiazoles (**8a-d**) were synthesized according to Scheme 1 by acylation of **3** with different acid chlorides followed by cyclization of the intermediates by means of Lawesson´s reagent.[25] The compounds **8e** and **8f-i** were synthesized in a one-pot manner. For that purpose, **3** was either condensed with carboxylic acid by means of dicyclohexylcarbodiimide and then treated with Lawesson´s reagent as done for **8e**, or reacted with the corresponding carboxylic acids and a mixture of Lawesson´s reagent and $POCl_3$ leading to compounds **8f-i**.

The thiazole **11** was prepared starting from **2** (Scheme 2). After conversion into the carboxylic acid chloride, the oxazole **9** was yielded by the reaction with isocyanoethylacetate and DBU. The hydrolyzation and decarboxylation led to the aminomethylketone **10**.[26] The thiazole **11** then resulted from the subsequent treatment of **10** with phenylpropionic acid, Lawesson´s reagent, $POCl_3$ and TEA.

The isomeric thiazole **13** was accessible through the reaction of benzimidazole-5(6)-carboxylic acid (**2**) with the aminomethylketone **12**, that was readily prepared from the respective carboxylic acid using carbonyldiimidazole, isocyanoethylacetate, DBU and aqueous HCl.

The 1,2,4-oxadiazole (**17**) and 1,2,4-triazole (**19**) were synthesized from 5(6)-Cyanobenzimidazole (**15**). **15** was treated either with hydroxylamine hydrochloride yielding N-hydroxybenzimidazole-5(6)-carboxamidine (**16**) or hydrazine hydrate, yielding the amidrazone **18** (Scheme 3). The latter was synthesized by a Pinner-reaction involving the imidatester as intermediate which was then converted into **18** by aminolysis with hydrazine hydrate. Both building blocks were acylated and cyclized in the same manner,[27] applying phenylpropionic acid and carbonyldiimidazole leading to the respective 1,2,4-oxadiazole- (**17**) or 1,2,4-triazole-substituted benzimidazole derivative (**19**).

The preparation of the 1,2,3-triazole-substituted benzimidazoles (**22a-d**, Scheme 4) started from 4-ethynyl-2-nitroaniline (**20**),[28,29] which was subjected to a click reaction that enabled a one-pot synthesis of the 1,2,3-triazole-substituted nitro-anilines (**21a-d**) applying different phenethyl-bromides.[30] **21a-d** were then converted into the corresponding benzimidazoles (**22a-d**) by reduction and cyclization using sodium formiate, palladium, formic acid and triethyl-orthoformiate.

Structure-Activity Relationship. Using **1a** (Fig. 2) as a starting point, the structure-activity relationship was investigated by the systematic modification of key scaffold elements: the central 5-membered heteroaromatic ring (Fig. 2: green), the spacer between the five-membered heteroaromatic ring and the terminal hydrophobic substituent (Fig. 2 yellow) as well as the substitution pattern at the hydrophobic substituent itself (Fig. 2: blue).

Initially, the pyridine-methylene-moiety was replaced by hydrophobic residues of different size and character (**5a-h**, Table1). This led to a minor improvement of the inhibitory potency as compared to **1a** only in case of the benzyl- and naphtyl-methyl-derivatives **5e** and **5f**. In contrast, the exchange of the pyridine-methylene substituent for plain aliphatic residues (**5a-5d**) resulted in a 5- to 20-fold decreased activity of the corresponding derivatives as compared to the starting point **1a**. Furthermore, keeping a terminal phenyl-moiety, the extension of the spacer length as in **5g-h** led to a decrease in the inhibitory potency in general. These findings led to the conclusion that a terminal phenyl moiety connected to the central five-membered heterocycle via a spacer of two heavy atoms length resembled the general shape and size of the inhibitory structure best.

Thus, the influence of this spacer on the inhibitory activity of the compounds was further explored. The exchange of the thio-ether present in **5e** by an amino-functionality (**6**, Table 2) led to a drop of potency, whereas the introduction of a methylene unit (**7a**) led to a slightly increased activity. Hence, this simplified analog was utilized as basis for further structural modifications. Furthermore, the exchange of the methylene unit proximate to the phenyl-moiety into an ether (**7b**) led to a decreased activity while the introduction of a sulfide (**7c**), or a sulfone (**7d**) was well tolerated and resulted in a doubled potency as compared to compound **7a**.

The impact of the central heterocycle on the activity of the compounds was also explored starting from the simplified analog **7a** (Table 3). Thereby the change of the central oxadiazole in **7a** into a thiadiazole (**8a**) resulted in a 2-times improvement of the inhibitory potency. The introduction of a thiazole resulted in a slight drop of potency in case of the 2-(benzimidazole-5(6)-yl)-thiazole (**13**) and a total loss of potency in case of the isomeric 5-(benzimidazole-5(6)-yl)-thiazole **11**. Also, the introduction of the 1,2,4-oxadiazole (**17**) or the 1,2,4-triazole (**19**) resulted in a moderate drop of potency. The potency of the 1,2,3-triazole **22a** was found to be 3-times higher as seen for **7a.**

Keeping the ethylene-spacer constant, the influence of the substitution pattern at the terminal phenyl moiety was investigated for the 1,3,4-oxadiazole as well as for the 1,3,4-thiadiazole derivatives (Table 4). Here, the introduction of electron-enriching methoxy-substituents in position 3 and 4 (**7e**, **8b**) or 2 and 3 (7**g**, **8d**) of the terminal phenyl, or their incorporation into a dioxolane-moiety (**7h**, **8e**) led to an improvement or perpetuation of the inhibitory potency, as compared to the un-substituted equivalents. A slight drop of potency resulted from the introduction of methoxy-substituents in the positions 2 and 4 of the phenyl ring (**7f**, **8c**). In all cases, the 1,3,4-thiadiazoles were found to be more potent as the corresponding 1,3,4-oxadiazoles, paralleling the findings with the un-substituted derivatives (Table 3). The introduction of electron-withdrawing fluoro- or trifluoro-methyl substituents as in 7**i**, **7j**, **7k**, **8f** and **8g** led to a decrease (**7i**, **7j**, **8f**) or a total loss of inhibitory potency (**7k**, **8g**). Since we observed an increased activity caused by electron-donating substituents, methoxy-substituents were also introduced to the 1,2,3-triazole derivative **22a**. This modification also led to an improved potency in case of the 4-methoxy-substituted derivative **22b** and the 3,4-dimethoxy derivative **22d**. However, the introduction of a methoxy-substituent in position 3 of the phenyl-moiety (**22c**) led to a slightly decreased activity compared to **22a**.

The combination of the above findings resulted in the most potent compounds of the study: **8h** and **8i** (Table 5). These compounds contained a central 1,3,4-thiadiazole and a terminal 3,4-dimethoxyphenyl moiety. Furthermore, the exchange of the methylene unit of the spacer proximate to the 3,4-dimethoxyphenyl substituent into a sulfide (**8h**) or sulfone (**8i**) led to an additional gain of potency, more pronounced for the sulfide-modification. Obviously, here the combination of a central 1,3,4-thiadiazole, the spacer modification and the introduction of the terminal 3,4-methoxyphenyl moiety summed up in a cooperative manner, resulting in a 40-fold and 12-fold improvement as compared to the starting compound **1a** for **8h** and **8i**, respectively.

Docking and mutagenesis studies. First information regarding the possible binding mode of this novel class of QC-inhibitors was gained by an *in-silico* docking analysis. This analysis was paralleled by an *in-vitro* mutagenesis study, in which the influence of the character of amino acid side chains in the active site on the inhibitory potency of selected compounds was evaluated. The two potent inhibitors, **8h** of the 1,3,4-thiadiazole series and **22b** of the 1,2,3-triazole series were selected for these studies.

The docking study was performed in consideration of the two different tautomeric forms of the metal-binding benzimidazole moiety, resulting in either 5- or 6-substituted derivatives of the inhibitors.

The results of the docking analysis, here exemplary shown for the results of the GoldScore® scoring function (for solutions of the other scoring functions see supporting information) and application of the PostDOCK script[31] are shown in Figure 3. The results of the fitness value for all 30 solutions are found in a range of 74.6 – 83.0 for the 6-yl tautomer and 79.1 – 87.0 in case of the 5-yl tautomer of **8h**. For compound **22b** this range was found within 70.4 – 78.0 for the 6-yl tautomer and within 78.2 – 84.0 for the respective 5-yl tautomer. In general, these findings could suggest a preferred binding of the 5-yl over the 6-yl tautomers. However, with the range of the scoring values being relatively narrow and differences between the single solutions being small, a certain pose of the inhibitors with a distinct minimum of binding energy cannot be concluded. Taking the uncertainty of scoring-functions in predicting binding-poses into account, all poses found have to be regarded as equally possible. However, taking a closer look on the results of the docking study, a pattern for the binding of the inhibitors is visible. In case of compound **8h**, when enabling the metal-contact of the benzimidazole-nitrogen leading to a 6-yl substituted inhibitor, all 30 docking-solutions are placed with the spacer-part and the terminal phenyl-moiety pointing towards a hydrophilic binding region formed by K144 and H206 (Fig 3A). Thereby the central 1,3,4-thiadiazole forms a π-π stacking interaction with the side chain of W207, located at the backside of the active-site opening. The solutions for the 5-yl isomer are almost equally distributed between two binding modes: one, occupying the hydrophilic binding region mentioned above, the other with the terminal phenyl residue part of the inhibitor adopting a hydrophobic binding area (Fig 3B) that is formed by the three amino acids I303, F325 and W329. A similar binding mode of an inhibitor was former identified by crystal structures of drosophila QC containing the first potent hQC inhibitor PBD150.[32] For compound **22b** the placement of the solutions is stricter, depending on which isomer of the metal-binding benzimidazole is considered. In all solutions for the 6-yl isomer, the phenyl-moiety of the compound is directed towards the hydrophilic binding region (Fig 3C), while almost all solutions of the 5-yl isomer are placed at the hydrophobic pocket (Fig 3D). Summing up, the docking experiments suggest two major ways of binding for each compound, which are differently populated, depending on which isomeric form of the inhibitor is considered.

For gaining a deeper insight in the likely "true" binding mode of the inhibitors, amino acids located at the active site and supposed to be involved in binding of the inhibitor molecules, were altered by *in-vitro* mutagenesis experiments. The effect of these changes on the potency of **8h** and **22b** was then elucidated by measurement of the inhibition constants for the mutant protein. A similar approach was recently published for the first potent QC-inhibitor PBD150.[33] According to the results of the above docking study, the amino-acids altered were either located in the hydrophobic region, as I303, F325 and W329 or in the hydrophilic region, as W207, H206 and K144 (Fig 3). The results of this study are summarized in Table 6. Clear changes in the inhibitory potency for both compounds **8h** and **22b** were visible for the mutagenesis of F325 and W329, as well as of W207. All other mutations did not remarkably affect the inhibitory potency. In the case of F325, the change of the aromatic side chain into the aliphatic, more polar asparagine or the aromatic and polar tyrosine led to a loss of the inhibitory potency for both tested inhibitors. In case of the aromatic W329, the inhibitory potency was maintained when a phenylalanine was placed in this position, but abolished, when a polar tyrosine was introduced. Also, the binding site at W207 was affected when its aromatic character was changed into the aliphatic leucine or glutamine. These findings can be interpreted in a way, that the binding of **8h** and **22b** in the hQC active site, besides the metal contact of the benzimidazole part, is enabled by interactions, maintained through F325, W329 and W207 (Fig 4).

The finding of the mutagenesis study would support the general binding mode for the 5-yl-benzimidazole isomers (Fig 3B and D) as suggested by docking. In these cases the aromatic moiety at the spacer end is bent towards the hydrophobic region. However, taking a closer look on the results, it turns out that none of the suggested solutions of the 5-yl tautomers of **8h** and **22b** does exactly match the results of the mutagenesis study. The majority of the docking solutions suggests an interaction with all three key amino-acids of the hydrophobic region, the mutagenesis study gives rise only for a contact with F325 and W329, leaving out I303. Also, the interaction of the inhibitor with W207, identified with the mutagenesis experiment, was not seen for the majority of docking solutions with the bent conformation. A π–π interaction of the central heterocycle was suggested only in those cases in which the spacer part with the terminal phenyl moiety pointed towards the pocket formed by H206 and K144.

The only exception showing a good match of the docking and the mutagenesis results was found in one single high ranking docking solution, but for a 6-yl tautomer and only in case of compound **22b**. In this single case a π–π interaction of the central heterocycle with W207 can be considered as well as an interaction of the terminal methoxy-phenyl moiety of **22b** with F325 and W329.

For a conclusive discussion of the possible binding mode of the new type of inhibitors in the active site of hQC the results of the analysis gained by mutagenesis study should be preferred over the ones suggested by docking. That is why the detailed analysis of the ligand-receptor interactions also in comparison to PBD150 is made based on the single docking result of **22b** mentioned above (see supporting information for details).

Conclusion. A new chemical class of inhibitors for human Glutaminyl Cyclase based on compounds identified by a ligand-based pharmacophore approach is presented. Thereby benzimidazole as a new metal-binding group is introduced. The optimization process, starting with inhibitors of a potency in the micromolar range, finally led to compounds with activities in the nanomolar range, with the most active compound **8h** exhibiting an inhibition constant of 23 nM. This result is in line with the most potent inhibitors of human Glutaminyl Cyclase known so far, that exhibit inhibitory constants between 60 and 6 nM.

Insight into the possible binding mode into the active site of hQC was gained by docking and mutagenesis studies. As the chemical structure of the new inhibitors can exist in two tautomeric forms, both, the 5-yl- as well as 6-yl substituted derivatives of the two potent representatives **8h** and **22b** were subjected to docking studies, resulting in the suggestion of two general binding modes. A site-directed mutagenesis approach identified amino acids in the active site that are involved in the inhibitor binding.

The comparison with the docking results indicated, that the inhibitors are likely to bind in the 5-yl substituted isomeric form, adopting a bent conformation. The most conclusive interpretation and best match of the mutagenesis and the docking experiments, however, was found for only one single docking solution of **22b** in its 6-yl tautomeric form. This means, a final conclusion on which tautomeric form of **22b** binds in the receptor cannot be drawn.

We consider the approach of combining docking studies with a site directed mutagenesis being a meaningful tool when, as seen here, docking studies are not conclusive and crystallographic data are not available for the molecules of interest. Further efforts towards the latter are now in focus of further investigations

Experimental Section.

Chemistry. Starting materials and solvents were purchased from Aldrich, Acros Organics, Alfa Aesar and Maybridge Co. The purity of the compounds was assessed by HPLC and confirmed to be ≥ 95%. The analytical HPLC-system consisted of a Merck-Hitachi device (model LaChrom®) utilizing a Phenomenex Luna 5 µM C18(2) column (125x4,0 mm) with λ = 214 nm as the reporting wavelength. The compounds were analyzed using a gradient at a flow rate of 1 mL/min; whereby eluent (A) was acetonitrile, eluent (B) was water, both containing 0.04 % (v/v) trifluoro acetic acid applying the following gradient: Method [A] 0 min – 25 min, 20-80% MeCN; 25 min – 30 min, 80-95% MeCN; 30 min -31 min, 95-20% MeCN; 31 min – 40 min, 20% MeCN; Method [B] 0 min – 15 min, 5-50% MeCN; 15 min – 20 min, 50-95% MeCN; 20 min -23 min, 95% MeCN; 23 min -24 min, 95-5% MeCN; 24 min – 30 min, 5% MeCN. The purities of all reported compounds were determined by the percentage of the peak area at 214 nm.

ESI-Mass spectra were obtained with a SCIEX API 150 and a SCIEX API 365 spectrometer (Perkin Elmer) utilizing the positive ionization mode. The high resolution positive ion ESI mass spectra were obtained from a Bruker Apex III 70e Fourier transform ion cyclotron resonance mass spectrometer (Bruker Daltonics, Billerica, USA) equipped with an Infinity™ cell. The melting points were detected utilizing a Kofler melting point device and are uncorrected. The ^{1}H NMR-Spectra were recorded at a VARIAN GEMINI 2000 (400 MHz) or at a BRUKER AC 500 (500 MHz). DMSO-D_6 was used as solvent unless otherwise specified. Chemical shifts are expressed as parts per million (ppm). The solvent was used as internal standard. Splitting patterns have been designated as follows: s (singulet), d (doublet), dd (doublet of doublet), t (triplet), m (multiplet) and br (broad signal). Semi preparative HPLC was performed on a Prepstar device (Varian) equipped with a Phenomenex Luna 10µM C18(2) column (250x21 mm). The compounds were eluted using the same solvent system as described above, applying a flow rate of 21 mL/min.

Benzimidazole-5(6)-carboxylic acid hydrazide 3

Step 1: **Benzimidazole-5(6)-carboxylic acid ethyl ester**: **2** (12.9 g; 80 mmol; 1 eq.) was dissolved in EtOH (200 ml), treated with conc. H_2SO_4 (5 ml; 88 mmol; 1.1 eq.) and heated to reflux for 24 h. After cooling to room temperature the mixture was poured into ice, basified by means of 5 N aqueous NaOH and extracted with EtOAc (3x100 ml). The combined organic layers were dried over Na_2SO_4 and evaporated. The remains were used without further purification. Yield: 12.6 g (82.9%); MS m/z: 191.3 $[M+H]^+$

Step 2: **Benzimidazole-5(6)-carboxylic acid hydrazide 3:** Benzimidazol-5(6)-carboxylic acid ethyl ester (12.6 g; 66 mmol; 1 eq.) was dissolved in EtOH (75 ml) and treated with $N_2H_4*H_2O$ (8.2 g; 264 mmol; 4 eq.). The mixture was heated to reflux for 48 h. The precipitate was collected by filtration after cooling, washed by means of heptane and used without further purification. Yield: 10.2 g (87.8%); MS m/z: 177.2 $[M+H]^+$

Benzimidazole-5(6)-(3H-1,3,4-oxadiazol-5-yl-2-thione) 4

Benzimidazole-5(6)-carboxylic acid hydrazide (9.0 g; 51 mmol; 1 eq.) was suspended in EtOH (85 ml). KOH (1.7 g; 30 mmol; 0.6 eq.) dissolved in water (17 ml) and CS_2 (3 ml; 50 mmol; 0.98 eq.) were added and the mixture was heated to reflux for 10 h. After cooling to room temperature the mixture was concentrated in vacuo and poured into ice. Concentrated $HCl_{(aq)}$ was added dropwise until a precipitate was formed. The solid was collected by filtration and used without further purification. Yield: 6.3 g (56.9%); MS m/z: 219.4 $[M+H]^+$

General procedure for the synthesis of the thioalkyl-substituted 1,3,4-oxadiazoles 5a-h

Benzimidazole-5(6)-(3H-1,3,4-oxadiazol-5-yl-2-thione) (330 mg; 1.5 mmol; 1 eq.) and triethylamine (0.209 ml; 1.5 mmol; 1 eq.) were dissolved in EtOH (10 ml). The respective alkylhalide (1.5 mmol; 1 eq.) was added and the mixture was heated to reflux over night. The solvent was evaporated and the residue was purified by flash chromatography on silica using a $CHCl_3$/MeOH gradient.

5(6)-(5-(4-Benzylamino)-1,3,4-oxadiazol-2-yl)benzimidazole 6

3 (0.354 g; 2 mmol; 1 eq.) was suspended in EtOH (20 ml). After addition of benzylisothiocyanate (298mg; 0.2 mmol; 1 eq.) the mixture was refluxed for 24 h. The solvent was evaporated and the residue was taken up in THF (30 ml). Dicyclohexylcarbodiimide (0.62 g; 3 mmol; 1.5 eq.) was added and the mixture was heated to reflux for 1 h. The solvent was evaporated and the remains were purified by flash chromatography on Al_2O_3 using a $CHCl_3$/MeOH gradient. Yield: 0.161 g (28.4%); mp: 109-111 °C; MS m/z: 292.4 $[M+H]^+$; ^{1}H-NMR, 500 MHz, DMSO d_6: δ 4.45 (d, 2H, ^3J=6.2 Hz); 7.25-7.28 (m, 1H); 7.33-7.36 (m, 2H); 7.39-7.40 (m, 2H); 7.67-7.71 (m, 2H); 7.97 (br s, 1H); 8.26 (t, 1H, ^3J=6.3 Hz); 8.33 (s, 1H); 12.69 (br s, 1H); ESI-FTICR-MS m/z: 292.11893 $[M+H]^+$; calc. for $C_{16}H_{14}N_5O^+$: 292.11929; HPLC (method B): rt 8.99 min (99.7%)

General procedure for the synthesis of the alkyl-substituted 1,3,4-oxadiazoles 7a, e-g

3 (176 mg; 1 mmol; 1 eq.) was suspended in THF (10 ml). Triethylamine (0.153 ml; 1.1 mmol; 1.1 eq.) and the respective acid chloride (1.1 mmol; 1.1 eq.) were added sequentially. After stirring at room temperature for 3 h the mixture was diluted by means water and extracted with EtOAc (3x25 ml). The combined organic layers were dried over Na_2SO_4 and evaporated. The residue was taken up in MeCN (10 ml), treated with $POCl_3$ (0.5 ml; 5.5 mmol; 5.5 eq.) and heated to reflux over night. After cooling the mixture was carefully basified by means of saturated aqueous $NaHCO_3$-solution and extracted with EtOAc (3x25 ml). The combined organic layers were dried over Na_2SO_4 and evaporated. The residue was purified by semi-preparative HPLC.

General procedure for the synthesis of the alkyl-substituted 1,3,4-oxadiazoles 7b-d, h-k

3 (176 mg; 1 mmol; 1 eq.) and the respective carboxylic acid were dissolved in $POCl_3$ (3 ml) and heated to reflux over night. After cooling the mixture was poured into ice water, basified by means of 2N aqueous NaOH and extracted with EtOAc (3x25 ml). The combined organic layers were dried over Na_2SO_4 and evaporated. The residue was purified by semi-preparative HPLC.

General procedure for the synthesis of the 1,3,4-thiadiazoles 8a-d

3 (176 mg; 1 mmol; 1 eq.) was suspended in THF (10 ml). Triethylamine (0.153 ml; 1.1 mmol; 1.1 eq.) and the respective acid chloride (1.1 mmol; 1.1 eq.) were added sequentially. After stirring at room temperature for 3 h the mixture was diluted by means of water and extracted with EtOAc (3x25 ml). The combined organic layers were dried over Na_2SO_4 and evaporated. The residue was taken up in THF (10 ml), treated with Lawesson´s reagent (606 mg; 1.5 mmol; 1.5 eq.) and heated to reflux for 1h. After cooling the mixture was diluted with water, basified by means of aqueous 2 N NaOH and extracted with EtOAc (3x25 ml). The combined organic layers were dried over Na_2SO_4 and evaporated. The remains were purified by flash chromatography on silica using a $CHCl_3$/MeOH gradient.

5(6)-(5-(2-(Benzo[d][1,3]dioxol-5-yl)ethyl)-1,3,4-thiadiazol-2-yl)benzimidazole 8e

3-(1,3-Benzodioxol-5-yl)propionic acid (195mg; 1 mmol; 1 eq.) was dissolved in THF (10 ml), treated with DCC (206 mg; 1 mmol; 1 eq.) and stirred at room temperature for 1h. Benzimidazole-5(6)-carboxylic acid hydrazide (176 mg; 1 mmol; 1 eq.) was added and the mixture was heated to 50°C over night. After cooling to room temperature, Lawesson´s reagent (606 mg; 1.5 mmol; 1.5 eq.) was added and the mixture was heated to reflux for 5h. After cooling to room temperature, the mixture was diluted by means of saturated aqueous $NaHCO_3$ solution and extracted with EtOAc (3x25 ml). The combined organic layers were dried over Na_2SO_4 and evaporated. The residue was purified by semi-preparative HPLC. Yield: 0.019 g (5.4%); mp: 125-128 °C; MS m/z: 351.3 $[M+H]^+$; ^{1}H-NMR, 400 MHz, DMSO d_6: δ 3.02 (t, 2H, ^3J=7.5 Hz); 3.42 (t, 2H, ^3J=7.5 Hz); 5.96 (s, 2H); 6.73 (dd, 1H, ^3J=7.9 Hz, ^4J=1.7 Hz); 6.81 (d, 1H, ^3J=7.9 Hz); 6.92 (d, 1H, ^4J=1.7 Hz); 7.83 (d, 1H, ^3J=8.3 Hz); 7.92 (dd, 1H, ^3J=8.3 Hz, ^4J=1.7 Hz); 8.22 (d, 1H, ^4J=1.7 Hz); 8.93 (s, 1H); ESI-FTICR-MS m/z: 351.09063 $[M+H]^+$; calc. for $C_{18}H_{15}N_4O_2S^+$: 351.09102; HPLC (method 2): rt 12.40 min (99.4%)

General procedure for the synthesis of the 1,3,4-thiadiazoles 8f-i

3 (176 mg; 1 mmol; 1 eq.) and the respective carboxylic acid (1 mmol; 1eq.) were suspended in MeCN (10 ml). Lawesson´s reagent (606 mg; 1.5 mmol; 1.5 eq.) and $POCl_3$ (0.137 ml; 1.5 mmol; 1.5 eq.) were added and the mixture was heated to reflux over night. After cooling to room temperature, the mixture was carefully basified by means of saturated aqueous $NaHCO_3$ solution and extracted with EtOAc (3x25 ml). The combined organic layers were dried over Na_2SO_4 and evaporated. The remains were purified by semi-preparative HPLC.

5-(Benzimidazole-5(6)-yl)oxazole-4-carboxylic acid ethylester 9

Benzimidazole-5(6)-carboxylic acid (1.62 g; 10 mmol; 1 eq.) was suspended in toluene (50 ml). Thionylchloride (3.63 ml; 50 mmol; 5 eq.) was added and the mixture was heated to reflux over night. After cooling the mixture was concentrated to dryness. The remains were resuspended in THF (50 ml), cooled to 0°C and treated with DBU (2.23 ml; 15 mmol; 1.5 eq.). A mixture of isocyanoethylacetate

(1.32 ml; 12 mmol; 1.2 eq.) and DBU (4.46 ml; 30 mmol; 3 eq.) in THF (50 ml) was added dropwise. After complete addition the reaction was allowed to warm to room temperature and stirring was continued for 24 h. The mixture was diluted by means of water and extracted with EtOAc (3x100 ml). The combined organic layers were dried over Na_2SO_4 and evaporated. The remains were purified by flashchromatography on silica using a $CHCl_3$/MeOH gradient. Yield: 2.0 g (78.0%); MS m/z: 258.3 $[M+H]^+$

Benzimidazole-5(6)-aminomethylketone-dihydrochloride 10

9 (2.0 g; 7.8 mmol) was dissolved in MeOH (20 ml). Concentrated aqueous HCl (40 ml) was added and the solution was heated to reflux over night. The solvent was evaporated to dryness and the residue was used without further purification. MS m/z: 176.3 $[M+H]^+$

5(6)-(2-Phenethylthiazol-5-yl)benzimidazole 11

10 (248 mg; 1 mmol; 1 eq.) and 3-Phenylpropionic acid (150 mg; 1 mmol; 1 eq.) were suspended in MeCN (10 ml). After addition of Lawesson´s reagent (606 mg; 1.5 mmol; 1.5 eq.), $POCl_3$ (0.137 ml; 1.5 mmol; 1.5 eq.) and triethylamine (0.22 ml; 3 mmol; 3 eq.) the mixture was heated to reflux over night. After cooling to room temperature the mixture was carefully diluted by means of saturated aqueous $NaHCO_3$ solution and extracted with EtOAc (3x25 ml). The combined organic layers were dried over Na_2SO_4 and evaporated. The remains were purified by semi-preparative HPLC. Yield: 0.025 g (8.2%); mp: 113-116 °C; MS m/z: 306.2 $[M+H]^+$; ^{1}H-NMR, 400 MHz, DMSO d_6: δ 3.09 (t, 2H, ^3J=7.5 Hz); 3.33 (t, 2H, ^3J=7.5 Hz); 7.18-7.21 (m, 1H); 7.28-7.29 (m, 4H); 7.71-7.73 (m, 1H); 7.80-7.82 (m, 1H); 7.93 (br s, 1H); 8.15 (s, 1H); 9.22 (br s, 1H); ESI-FTICR-MS m/z: 306.10634 $[M+H]^+$; calc. for $C_{18}H_{16}N_3S^+$: 306.10594; HPLC (method B): rt 13.00 min (100%).

Amino-4-phenylbutan-2-on-hydrochloride 12

Phenylpropionic acid (451 mg; 3 mmol; 1 eq.) was dissolved in THF (10 ml), treated with CDI (486 mg; 3 mmol; 1 eq.) and stirred at room temperature for 1 h. The mixture was cooled to 0°C and a mixture of isocyanoethylacetate (0.393 ml; 3.6 mmol; 1.2 eq.) and DBU (1.34 ml; 9 mmol; 3 eq.) in THF (10 ml) was added dropwise. After complete addition, the mixture was stirred at room temperature for 24 h. After dilution by means of water, the mixture was extracted with EtOAc (3x25 ml). The combined organic layers were dried over Na_2SO_4 and evaporated. The remains were purified by flashchromatography on silica using a $CHCl_3$/MeOH gradient. Yield: 319 mg (43.4%); MS m/z: 246.3 $[M+H]^+$.

The residue was dissolved in MeOH (5 ml), treated with aqueous concentrated HCl (15 ml) and heated to reflux over night. The solvent was evaporated to dryness. The compound was used without further purification. MS m/z: 164.4 $[M+H]^+$;

5(6)-(5-Phenethylthiazol-2-yl)benzimidazole 13

The compound was synthesized from Amino-4-phenylbutan-2-on-hydrochloride (**12**; 163 mg) and **2** (162 mg) according to the method described for **11**. Yield: 0.042 g (13.8%); mp: 109-111 °C; MS m/z: 306.1 $[M+H]^+$; ^{1}H-NMR, 400 MHz, DMSO d_6: δ 2.98 (t, 2H, ^3J=7.5 Hz); 3.20 (t, 2H, ^3J=7.5 Hz); 7.17-7.22 (m, 1H); 7.25-7.31 (m, 4H); 7.62 (s, 1H); 7.80 (d, 1H, ^3J=8.7 Hz); 7.90 (dd, 1H, ^3J=8.3 Hz, ^4J=1.7 Hz); 8.16 (d, 1H, ^4J=1.7 Hz); 9.02 (s, 1H); ESI-FTICR-MS m/z: 306.10603 $[M+H]^+$; calc. for $C_{18}H_{16}N_3S^+$: 306.10594; HPLC (method B): rt 13.73 min (97.4%)

5(6)-Cyanobenzimidazole 15

14 (5.0 g; 37 mmol; 1 eq.) was dissolved in 5 N aqueous HCl (200 ml). After addition of formic acid (20 ml) the mixture was heated to reflux for 3 h. After cooling the mixture was basified by means of aqueous ammonia and stored in a fridge over night. The formed precipitate was collected by filtration, washed with water and used without further purification. Yield: 3.6 g (67.6%); MS m/z: 144.2 $[M+H]^+$

N-Hydroxy-benzimidazole-5(6)-carboxamidine 16

A solution of 5(6)-cyanobenzimidazole (1.43 g; 10 mmol; 1 eq.) in EtOH (30 ml) was treated with K_2CO_3 (2.76 g; 20 mmol; 2 eq.) and H_2NOH*HCl (0.77 g; 11 mmol; 1.1 eq.) and heated to reflux over night. After cooling to room temperature the mixture was diluted by means of diethylether. The precipitate was collected by filtration, washed with water and dried in vacuo. The compound was used without further purification. Yield: 1.28 g (72.7%); MS: 177.3 $[M+H]^+$

5(6)-(5-Phenethyl-1,2,4-oxadiazol-3-yl)benzimidazole 17

3-Phenylpropionic acid (150 mg; 1 mmol; 1 eq.) was dissolved in DMF (5 ml), treated with carbonyldiimidazole (162 mg; 1 mmol; 1 eq.) and stirred at room temperature for 1h. After addition of **16** (176 mg; 1 mmol; 1eq.) the temperature was increased to 110°C and stirring was continued over night. After cooling the mixture was diluted by means of water and saturated aqueous $NaHCO_3$ solution and extracted with EtOAc (3x25 ml). The combined organic layers were dried over Na_2SO_4 and evaporated. The remains were purified by flash chromatography on silica using a $CHCl_3$/MeOH gradient. Yield: 0.053 g (18.3%); mp: 109-110 °C; MS m/z: 291.3 $[M+H]^+$; ^{1}H-NMR, 400 MHz, DMSO d_6: δ 3.15 (t, 2H, ^3J=7.9 Hz); 3.33 (t, 2H, ^3J=7.9 Hz); 7.18-7.22 (m, 1H); 7.27-7.30 (m, 4H); 7.66-7.87 (br m, 2H), 8.15-8.24 (br m, 1H); 8.34-8.36 (m, 1H); 12.69-12.72 (m, 1H); ESI-FTICR-MS m/z: 291.12362 $[M+H]^+$; calc. for $C_{17}H_{15}N_4O^+$: 291.12404; HPLC (method B): rt 13.21 min (99.1%)

Benzimidazole-5(6)-carboxamidrazone 18

Gaseous HCl was bubbled through an ice cooled solution of **15** (1.43 g; 10 mmol; 1 eq.) in dry EtOH (20 ml). The tube was sealed and stirred at room temperature for 48 h. The mixture was diluted by means of diethylether. The precipitate was collected by filtration, washed with a small amount of EtOH and dietyhlether and was dried in vacuo. The residue was resuspended in EtOH (20 ml), treated with N_2H_4*H_2O (1.5 g; 30 mmol; 3 eq.) and stirred at room temperature for 3 h. The precipitate was collected by filtration and washed by means of water. The residue was used without further purification. Yield: 0.75 g (42.9%); MS m/z: 176.4 $[M+H]^+$

5(6)-(5-Phenethyl-4H-1,2,4-triazol-3-yl)benzimidazole 19

A solution of 3-Phenylpropionic acid (150 mg; 1 mmol; 1 eq.) in DMF (5 ml) was treated with carbonyldiimidazole (162 mg; 1 mmol; 1 eq.) and stirred at room temperature for 1 h. After addition of **18** (175 mg; 1 mmol; 1 eq.) the temperature was increased to 110°C and stirring was continued for 24h. The mixture was cooled to room temperature, diltuted by means of water and saturated aqueous $NaHCO_3$ solution and extracted with EtOAc (3x25 ml). The combined organic layers were dried over Na_2SO_4 and evaporated. The remains were purified by flash chromatography on silica using a $CHCl_3$/MeOH gradient. Yield: 0.062 g (21.5%); mp: 115-119 °C; MS m/z: 290.1 $[M+H]^+$; 145.8 $[M+2H]^{2+}$; ^{1}H-NMR, 400 MHz, DMSO d_6: δ 2.94 (br s, 2H); 3.30 (br s, 2H); 7.00 (s, 1H); 7.25-7.28 (m, 4H); 7.59-7.65 (m, 1H); 7.85-7.87 (m, 1H); 8.16-8.30 (m, 1H); ESI-FTICR-MS m/z: 290.14006 $[M+H]^+$; calc. for $C_{17}H_{16}N_5^+$: 290.14002; HPLC (method B): rt 10.06 min (100%)

4-Ethinyl-2-nitroaniline 20

The compound was synthesized as described in:[28,29]

Step 1: 2-Nitro-4-(trimethylsilylethinyl)aniline: A solution of 4-iodo-2-nitroaniline (5.32 g; 20 mmol; 1 eq.) in THF (20 ml) was treated with $PdCl_2(PPh_3)_2$ (154 mg; 0.22 mmol; 0.011 eq.), CuI (84 mg; 0.44 mmol; 0.022 eq.) and DIPEA (10.5 ml; 60 mmol; 3 eq.) under argon atmosphere. Trimethylsilylacetylene (3.1 ml; 22 mmol; 1.1 eq.) was added drop-wise at room temperature. After complete addition, stirring was continued for 3h. The mixture was diluted by means of water and extracted with EtOAc (3x100 ml). The combined organic layers were dried over Na_2SO_4 and evaporated. The remains were purified by flash chromatography on silica using a $CHCl_3$/MeOH gradient. Yield: 3.96 g (84.6%); MS m/z: 235.3 $[M+H]^+$; 469.4 $[2M+H]^+$

Step 2: 4-Ethinyl-2-nitroaniline 20: A solution of 2-nitro-4-(trimethylsilylethinyl)aniline (3.96 g; 16.9 mmol; 1 eq.) in MeOH/CH_2Cl_2 (100 ml; 1:1 v/v) was treated with K_2CO_3 (9.33 g; 67.6 mmol; 4 eq.). The mixture was stirred at room temperature for 5 h. After dilution by means of water, the organic layer was separated. The aqueous layer was extracted with CH_2Cl_2 (2x100 ml). The combined organic layers were dried over Na_2SO_4 and evaporated. The remains were purified by flash chromatography on silica using a $CHCl_3$/MeOH gradient. Yield: 2.06 g (75.1%); MS m/z: 163.4 $[M+H]^+$

General procedure for the synthesis of the 4-(1-Alkyl-1,2,3-triazol-4-yl)-2-nitroanilines 21a-d

Sodium azide (65 mg; 1 mmol; 1 eq.) was dissolved in DMSO (2 ml), treated with the respective alkylbromide (1 mmol; 1 eq.) and stirred at room temperature for 24h. The mixture was diluted with water (2 ml), treated with sodium ascorbate (20 mg; 0.1 mmol; 0.1 eq.), **20** (162 mg; 1 mmol; 1 eq.) and an aqueous 1 M solution of $CuSO_4$*5 H_2O (0.2 ml; 2 mmol; 0.2 eq.) and stirred at room temperature for 3h. The formed precipitate was collected by filtration, washed by means of water and dried in vacuo. The residue was used without further purification.

General procedure for the synthesis of the 1,2,3-triazoles 22a-d

A solution of the respective 4-(1-Alkyl-1,2,3-triazol-4-yl)-2-nitroaniline in formic acid and triethylorthoformiate (10 ml; 1:1 v/v) was treated with sodium formiate (2.04 g; 30 mmol) and palladium on charcoal. The sealed tube was heated to 110°C for 24h. After cooling to room temperature the mixture was filtered through Celite and concentrated in vacuo. The residue was redissolved in water, basified by means of aqueous saturated $NaHCO_3$ solution an extracted with EtOAc (3x25 ml). The combined organic layers were dried over Na_2SO_4 and evaporated. The remains were purified by flash chromatography on silica using a $CHCl_3$/MeOH gradient.

Computational Chemistry

For the flexible alignment of PBD150 and the substrate H-Gln-Phe-Ala-NH_2 the Molecular Operating Environment (MOE) in the version 2003.02 was used (Chemical Computing Group, Montreal, Canada). For the pharmacophore search itself and for the visualization of the docking results MOE in the version 2011.10 was used. Molecular Docking was done by using GOLD vers. 5.0 (CCDC Software Ltd., Cambridge, U.K.).

Flexible Alignment and Pharmacophore search. The flexible alignment of H-Gln-Phe-Ala-NH_2, 1-(3-(1*H*-Imidazol-1yl-)propyl)-3-(3,4-dimethoxyphenyl)thiourea (PBD150) and N-(3-(1*H*-Imidazol-1-yl)propyl)-1-(3,4-dimethoxyphenyl)cyclopropanecarbothioamide was accomplished as described elsewhere[17]. After sorting the list concerning the average energies, the alignment on position 37 (U = -4.32 kcal/mol, S = 97.91) was used for the pharmacophore creation. Thereby the pharmacophore editor was opened and the pharmacophore was built as follows by using the PCH_All scheme: **F1:** Metal ligator & "[n]1ccnc1", R=1.2, essential: yes, N3 of the imidazole moiety of PBD150; **F2:** Acceptor, R=1.2, essential: no, sulfur of the thiourea moiety of PBD150; **F3**: Donor, R=1.2, essential: no, N of the thioamide moiety of the corresponding derivative, **F4:** Aromatic|Hydrophobic, R=1.4, essential: no, center of the phenyl side chain of H-Gln-Phe-Ala-NH_2; **F5:** Acceptor, R=1.1, essential: no, oxygen of the 4-methoxygroup of PBD150. Compounds had to fulfill at least 4 of the 5 features. The search was done by using the pre-processed databases "leadlike_conf_001.mdb" – "leadlike_conf_008.mdb" that are provided with the MOE-package. They contain more than 650.000 chemical structures that are pre-filtered concerning the criteria of Oprea et al. [20,21] including their conformational space. After this the compounds were successively filtered for compounds containing a benzimidazole as substructure and the TPSA-value below or equal to 70 Å^2. The remaining compounds were analyzed for there commercially availability and their synthetic access, resulting in 69 compounds that were tested using the assay described below. The compounds sharing in this paper as the starting point for further chemical exploration were purchased from Asinex (**1a**: ASN6346968; **1b**: ASN6346970; **1c**: ASN06346980)..

Docking. For the molecular docking of the compounds **8h** and **22b** the pdb file 3si0 (www.rcsb.org) was used. Thereby the protonate 3D functionality of MOE® (vers. 2011.10) was applied in order to protonate the system. The co-crystallized imidazole was removed from the system. After the protein file was converted into the mol2-format the subsequent steps were performed in GOLD®. Any water outside the active site was removed. All remaining water molecules were set to toggle. The active site was defined using the zinc as the center with a radius of 15 Å. A substructure constraint for the benzimidazole moiety as the metal binding group was used, with a force constant of 10. Both tautomeric forms of the inhibitors were created in MOE, energy minimized and saved as mol2 file. The resulting 4 compounds were then docked 30 times applying each of the available scoring functions. The solutions for each tautomer and scoring function with the corresponding score values were converted into MOE databases, applying a svl-script provided by CCG. The postdock-1.2.svl script, available via the svl exchange server (svl.chemcomp.com), was used to create the corresponding figures.

Biochemistry

Inhibitor Testing. QC activity was assayed essentially as described in[34]. For a fluorometric detection the assay consisted of varying concentrations of H-Gln-AMC (7-amino-4-methylcoumarin, Bachem, Bubendorf, Switzerland) in a concentration range between 0.25 and 4 K_m in 50 mM Tris-HCl, pH 8.0; 0.4 $^{U}/_{ml}$ recombinant pyroglutamyl aminopeptidase (pGAP) from *Bacillus amyloliqefaciens* (Qiagen, Hilden, Germany) as auxiliary enzyme and the inhibitory compound. For excitation/emission a wavelength of 380/460 nm (H-Gln-AMC) was used. Reactions were started by addition of QC. The activity was determined from a standard curve of the fluorophore under assay conditions. All determinations were carried out at 30°C by using a BMG Fluostar reader for microplates (BMG Labtechnologies, Offenburg, Germany). Evaluation of all kinetic data was performed with GraFit as the analyzing software (version 5.0.4. for windows, ERITHACUS SOFTWARE Ltd., Horley, UK).

Mutagenesis. Cloning, expression and purification of hQC and the diverse variants were performed as previously described.[33] For all cloning procedures the Escherichia coli strain DH5α was applied. The hQC cDNA was inserted into the yeast expression vector pPICZαB (Invitrogen, Karlsruhe, Germany) with additionally introduction of an N-terminal His6-tag (primer pair Cs/Cas, Table S1). The mutations in hQC cDNA were introduced according to the quik-change II site-directed mutagenesis protocol (Stratagene, Santa Clara, CA, USA) using appropriate primer pairs (Table S1). The cDNA was verified by sequencing (primer Ss, Sas for K144 mutation, Table S1). Plasmid DNA was amplified, purified (Plasmid Miniprep Kit, Qiagen, Hilden, Germany) and linearized (Pme1 endonuclease).

For heterologous target protein expression strain X33 (AOX1, AOX2) of the methylotrophic yeast Pichia pastoris was used. Yeast was grown, transformed and analyzed according to the manufacturer's instructions (Invitrogen, Karlsruhe, Germany). Transformation of competent yeast cells was performed by electroporation according to the manufacturer's instructions (Bio-Rad, Munich, Germany). Transgenics were screened for target protein expression. Clones displaying highest QC activity were chosen for large expression. To confirm the insertion of the correct hQC variant, genomic DNA was prepared according to standard molecular biological techniques. The target DNA was amplified by PCR using gene specific primer pairs flanking the mutation site and the sequence was analyzed.

For large scale expression, high cell density fermentation in a 5 l reactor (Biostad B; Braun Biotech, Melsungen, Germany) or expression in shake flasks were applied, essentially as described elsewhere.[35,36] The purification of hQC variants followed three liquid chromatographic steps: Ni^{2+}-IMAC (immobilized metal affinity chromatography), hydrophobic interaction and anion exchange chromatography.[36] QC-containing fractions were pooled and purity was analyzed by SDS-PAGE (sodium dodecyl sulfate polyacrylamide gel electrophoresis, Servagel TG 4-20, Serva, Heidelberg, Germany) and Coomassie Blue staining. The purified enzyme was stored at -20°C after addition of glycerol [50% (V/V)] or without glycerol at -80°C.

Acknowledgment. The authors are grateful for helpful discussions with Stephan Schilling. We thank Antje Hamann and Ulf-Torsten Gärtner for technical synthesis support as well as Guido Kirsten and Markus Kossner (Chemical Computing Group) for providing useful svl-scripts.

Supporting Information Available. Compound data, detailed experimental data of the mutagenesis study and the docking experiments are available free of charge via the Internet at http://pubs.acs.org.

ABBREVIATIONS. hQC, human Glutaminyl Cyclase; pGlu, *pyro*-glutamyl; MBG, metal-binding-group.

*To whom correspondence should be addressed. Phone: +49 (0) 345 5559908. Fax: +49 (0) 345 5559901. E-mail: ulrich.heiser@probiodrug.de

REFERENCES.

(1) Awadé, A. C.; Cleuziat, P.; GonzalèS, T.; Robert-Baudouy, J. Pyrrolidone carboxyl peptidase (Pcp): An enzyme that removes pyroglutamic acid (pGlu) from pGlu-peptides and pGlu-proteins. *Proteins* **1994**, *20*, 34–51.

(2) Abraham, G. Pyroglutamic acid. *Mol. Cell. Biochem.* **1981**, *38*, 181–190.

(3) Van Coillie, E.; Proost, P.; Van Aelst, I.; Struyf, S.; Polfliet, M.; De Meester, I.; Harvey, D. J.; Van Damme, J.; Opdenakker, G. Functional comparison of two human monocyte chemotactic protein-2 isoforms, role of the amino-terminal pyroglutamic acid and processing by CD26/dipeptidyl peptidase IV. *Biochemistry* **1998**, *37*, 12672–12680.

(4) Busby, W. H.; Quackenbush, G. E.; Humm, J.; Youngblood, W. W.; Kizer, J. S. An enzyme(s) that converts glutaminyl-peptides into pyroglutamyl-peptides. Presence in pituitary, brain, adrenal medulla, and lymphocytes. *J. Biol. Chem.* **1987**, *262*, 8532–8536.

(5) Cynis, H.; Rahfeld, J.-U.; Stephan, A.; Kehlen, A.; Koch, B.; Wermann, M.; Demuth, H.-U.; Schilling, S. Isolation of an Isoenzyme of Human Glutaminyl Cyclase: Retention in the Golgi Complex Suggests Involvement in the Protein Maturation Machinery. *J. Mol. Biol.* **2008**, *379*, 966–980.

(6) Pohl, T.; Zimmer, M.; Mugele, K.; Spiess, J. Primary structure and functional expression of a glutaminyl cyclase. *Proc. Natl. Acad. Sci. U.S.A.* **1991**, *88*, 10059–10063.

(7) Böckers, T. M.; Kreutz, M. R.; Pohl, T. Glutaminyl-cyclase expression in the bovine/porcine hypothalamus and pituitary. *J. Neuroendocrinol.* **1995**, *7*, 445–453.

(8) Gunn, A. P.; Masters, C. L.; Cherny, R. A. Pyroglutamate-Abeta: Role in the natural history of Alzheimer's disease. *Int. J. Biochem. Cell Biol.* **2010**, 1–4.

(9) Jawhar, S.; Wirths, O.; Bayer, T. A. Pyroglutamate-Aβ: A Hatchet Man in Alzheimer Disease. *J. Biol. Chem.* **2011**, *286*, 38825–38832.

(10) Schilling, S.; Lauber, T.; Schaupp, M.; Manhart, S.; Scheel, E.; Böhm, G.; Demuth, H.-U. On the Seeding and Oligomerization of pGlu-Amyloid Peptides (in vitro). *Biochemistry* **2006**, *45*, 12393–12399.

(11) Schlenzig, D.; Manhart, S.; Cinar, Y.; Kleinschmidt, M.; Hause, G.; Willbold, D.; Funke, S. A.; Schilling, S.; Demuth, H.-U. Pyroglutamate Formation Influences Solubility and Amyloidogenicity of Amyloid Peptides. *Biochemistry* **2009**, *48*, 7072–7078.

(12) Nussbaum, J. M.; Schilling, S.; Cynis, H.; Silva, A.; Swanson, E.; Wangsanut, T.; Tayler, K.; Wiltgen, B.; Hatami, A.; Rönicke, R.; Reymann, K.; Hutter-Paier, B.; Alexandru, A.; Jagla, W.; Graubner, S.; Glabe, C. G.; Demuth, H.-U.; Bloom, G. S. Prion-like behaviour and tau-dependent cytotoxicity of pyroglutamylated amyloid-β. *Nature* **2012**, 1–5.

(13) Jawhar, S.; Wirths, O.; Schilling, S.; Graubner, S.; Demuth, H.-U.; Bayer, T. A. Overexpression of glutaminyl cyclase, the enzyme responsible for pyroglutamate A{beta} formation, induces behavioral deficits, and glutaminyl cyclase knock-out rescues the behavioral phenotype in 5XFAD mice. *J. Biol. Chem.* **2011**, *286*, 4454–4460.

(14) Alexandru, A.; Jagla, W.; Graubner, S.; Becker, A.; Bäuscher, C.; Kohlmann, S.; Sedlmeier, R.; Raber, K. A.; Cynis, H.; Rönicke, R.; Reymann, K. G.; Petrasch-Parwez, E.; Hartlage-Rübsamen, M.; Waniek, A.; Rossner, S.; Schilling, S.; Osmand, A. P.; Demuth, H.-U.; Hörsten, von, S. Selective hippocampal neurodegeneration in transgenic mice expressing small amounts of truncated Aβ is induced by pyroglutamate-Aβ formation. *J. Neurosci.* **2011**, *31*, 12790–12801.

(15) Schilling, S.; Appl, T.; Hoffmann, T.; Cynis, H.; Schulz, K.; Jagla, W.; Friedrich, D.; Wermann, M.; Buchholz, M.; Heiser, U.; Hrsten, von, S.; Demuth, H.-U. Inhibition of glutaminyl cyclase prevents pGlu-A formation after intracorticalhippocampal microinjection in vivoin situ. *J. Neurochem.* **2008**, *106*, 1225–1236.

(16) Schilling, S.; Zeitschel, U.; Hoffmann, T.; Heiser, U.; Francke, M.; Kehlen, A.; Holzer, M.; Hutter-Paier, B.; Prokesch, M.; Windisch, M.; Jagla, W.; Schlenzig, D.; Lindner, C.; Rudolph,

T.; Reuter, G.; Cynis, H.; Montag, D.; Demuth, H.-U.; Rossner, S. Glutaminyl cyclase inhibition attenuates pyroglutamate Aβ and Alzheimer's disease–like pathology. *Nat. Med.* **2008**, *14*, 1106–1111.

(17) Buchholz, M.; Heiser, U.; Schilling, S.; Niestroj, A. J.; Zunkel, K.; Demuth, H.-U. The First Potent Inhibitors for Human Glutaminyl Cyclase: Synthesis and Structure−Activity Relationship. *J. Med. Chem.* **2006**, *49*, 664–677.

(18) Buchholz, M.; Hamann, A.; Aust, S.; Brandt, W.; Böhme, L.; Hoffmann, T.; Schilling, S.; Demuth, H.-U.; Heiser, U. Inhibitors for Human Glutaminyl Cyclase by Structure Based Design and Bioisosteric Replacement. *J. Med. Chem.* **2009**, *52*, 7069–7080.

(19) Molecular Operating Environment (MOE) 2011.10. *Chemical Computing Group Inc, 1010 Sherbooke St West, Suite #910, Montreal, QC, Canada, H3A 2R7* **2011**.

(20) Oprea, T. I.; Davis, A. M.; Teague, S. J.; Leeson, P. D. Is There a Difference between Leads and Drugs? A Historical Perspective. *J. Chem. Inf. Model.* **2001**, *41*, 1308–1315.

(21) Oprea, T. I. Property distribution of drug-related chemical databases. *J. Comput. Aided Mol. Des.* **2000**, *14*, 251–264.

(22) Parra, M.; Belmar, J.; Zunza, H. 2, 5□Disubstituted 1, 3, 4□Oxadiazoles: Synthesis and mesomorphic behaviour. *J. Prakt. Chem.* **1995**, *337*, 239–241.

(23) Labouta, I. M.; Hassan, A. M. M.; Aboulwafa, O. M.; Kader, O. Synthesis of some substituted benzimidazoles with potential antimicrobial activity. *Monatsh. Chem.* **1989**, *120*, 571–574.

(24) Roy, R. U.; Desai, A. R.; Desai, K. R. Synthesis and antimicrobial activity of 1,2,4-triazoles. *E-J. Chem.* **2005**, *2*, 1–5.

(25) Alker, D.; Campbell, S. F.; Cross, P. E.; Burges, R. A.; Carter, A. J.; Gardiner, D. G. Long-acting dihydropyridine calcium antagonists. 3. Synthesis and structure-activity relationships for a series of 2-[(heterocyclylmethoxy)methyl] derivatives. *J. Med. Chem.* **1989**, *32*, 2381–2388.

(26) Armaregoa, W. L. F.; Taguchib, H.; Cottonc, R. G. H.; Battistona, S.; Leong, L. Lipophilic 5,6,7,8-tetrahydropterin substrates for phenylalanine hydroxylase (monkey brain), tryptophan hydroxylase (rat brain) and tyrosine hydroxylase (rat brain). *Eur. J. Med. Chem.* **1987**, *22*, 283–291.

(27) Koo, K. D.; Kim, M. J.; Kim, S.; Kim, K.-H.; Hong, S. Y.; Hur, G.-C.; Yim, H. J.; Kim, G. T.; Han, H. O.; Kwon, O. H. Synthesis, SAR, and X-ray structure of novel potent DPPIV inhibitors: Oxadiazolyl ketones. *Bioorg. Med. Chem. Lett.* **2007**, *17*, 4167–4172.

(28) Maya, F.; Chanteau, S. H.; Cheng, L.; Stewart, M. P.; Tour, J. M. Synthesis of Fluorinated Oligomers toward Physical Vapor Deposition Molecular Electronics Candidates. *Chem. Mater.* **2005**, *17*, 1331–1345.

(29) Price, D. Improved and new syntheses of potential molecular electronics devices. *Tetrahedron* **2003**, *59*, 2497–2518.

(30) Kacprzak, K. Efficient One-Pot Synthesis of 1,2,3-Triazoles from Benzyl and Alkyl Halides. *Synlett* **2005**, 0943–0946.

(31) Springer, C.; Adalsteinsson, H.; Young, M. M.; Kegelmeyer, P. W.; Roe, D. C. PostDOCK: A Structural, Empirical Approach to Scoring Protein Ligand Complexes. *J. Med. Chem.* **2005**, *48*, 6821–6831.

(32) Koch, B.; Kolenko, P.; Buchholz, M.; Ruiz Carrillo, D.; Parthier, C.; Wermann, M.; Rahfeld, J.-U.; Reuter, G.; Schilling, S.; Stubbs, M. T.; Demuth, H.-U. Crystal Structures of Glutaminyl Cyclases (QCs) from Drosophila melanogaster Reveal Active Site Conservation between Insect and Mammalian QCs. *Biochemistry* **2012**, *51*, 7383–7392.

(33) Koch, B.; Buchholz, M.; Wermann, M.; Heiser, U.; Schilling, S.; Demuth, H.-U. Probing Secondary Glutaminyl Cyclase (QC) Inhibitor Interactions Applying an in silico-Modeling/Site-Directed Mutagenesis Approach: Implications for Drug Development. *Chem. Biol. Drug Des.* **2012**, *80*, 937–946.

(34) Schilling, S.; Hoffmann, T.; Wermann, M.; Heiser, U.; Wasternack, C.; Demuth, H.-U. Continuous Spectrometric Assays for Glutaminyl Cyclase Activity. *Anal. Biochem.* **2002**, *303*,

49–56.
(35) Schilling, S.; Hoffmann, T.; Rosche, F.; Manhart, S. Heterologous expression and characterization of human glutaminyl cyclase: evidence for a disulfide bond with importance for catalytic activity. *Biochemistry* **2002**.
(36) Ruiz Carrillo, D.; Koch, B.; Parthier, C.; Wermann, M.; Dambe, T.; Buchholz, M.; Ludwig, H.-H.; Heiser, U.; Rahfeld, J.-U.; Stubbs, M. T.; Schilling, S.; Demuth, H.-U. Structures of Glycosylated Mammalian Glutaminyl Cyclases Reveal Conformational Variability near the Active Center. *Biochemistry* **2011**, *50*, 6280–6288.

Table 1.

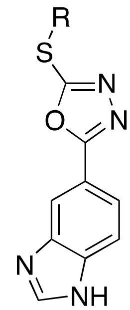

entry	R	IC_{50} [μM]	K_i [μM]	entry	R	IC_{50} [μM]	K_i [μM]
5a	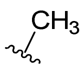	24.80	17.8 ± 0.35	**5e**	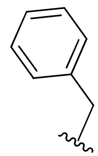	4.24	0.78 ± 0.07
5b	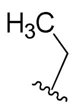	14.70	9.67 ± 0.02	**5f**	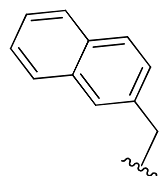	8.67	0.60 ± 0.03
5c	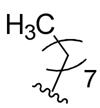	15.00	n.d.	**5g**	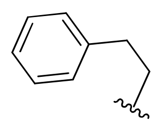	7.26	6.07 ± 0.46
5d	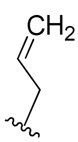	7.23	5.26 ± 0.19	**5h**	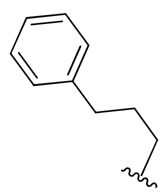	7.56	4.56 ± 0.17

Table 2.

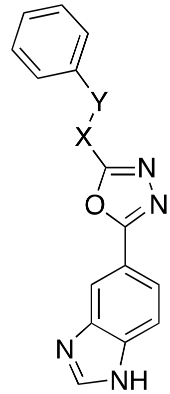

entry	X	Y	IC_{50} [µM]	K_i [µM]
6	NH	CH_2	28.13	4.87 ± 0.29
7a	CH_2	CH_2	3.96	0.638 ± 0.015
7b	CH_2	O	4.28	0.941 ± 0.038
7c	CH_2	S	1.27	0.351 ± 0.011
7d	CH_2	SO_2	1.86	0.335 ± 0.016

Table 3.

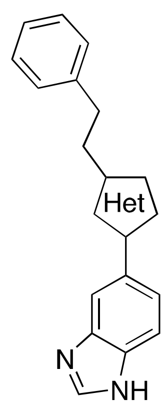

entry	Het	IC_{50} [µM]	K_i [µM]
7a	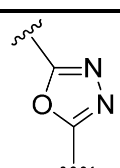	3.96	0.638 ± 0.015

8a	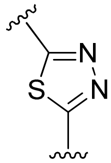	2.38	0.333 ± 0.018
11	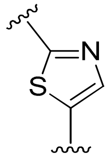	24.70	n.d.
13	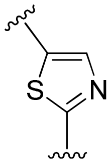	5.05	1.310 ± 0.080
17	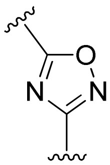	4.50	1.250 ± 0.039
19	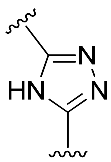	4.56	1.040 ± 0.037
22a	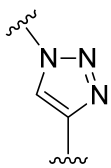	1.59	0.211 ± 0.007

Table 4.

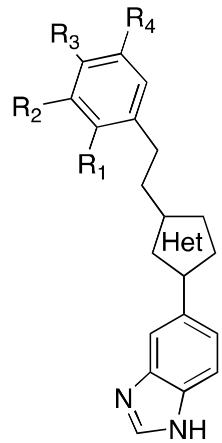

entry	Het	R_1	R_2	R_3	R_4	IC_{50} [μM]	K_i [μM]
7e		H	OCH_3	OCH_3	H	2.33	0.424 ± 0.008
7f		OCH_3	H	OCH_3	H	3.13	0.716 ± 0.017
7g		OCH_3	OCH_3	H	H	1.91	0.382 ± 0.010
7h	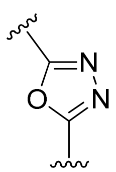	H	-OCH_2O-		H	2.65	0.415 ± 0.095
7i		F	H	F	H	4.48	0.702 ± 0.017
7j		H	H	CF_3	H	7.30	1.140 ± 0.053
7k		CF_3	H	H	CF_3	26.90	n.d.
8b		H	OCH_3	OCH_3	H	0.73	0.107 ± 0.005
8c		OCH_3	H	OCH_3	H	2.99	0.645 ± 0.028
8d	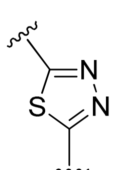	OCH_3	OCH_3	H	H	0.70	0.157 ± 0.005
8e		H	-OCH_2O-		H	0.99	0.167 ± 0.003
8f		F	H	F	H	2.23	0.536 ± 0.014

8g		H	H	CF_3	H	31.70	n.d.
22b		H	H	OCH_3	H	0,63	0,106 ± 0,003
22c	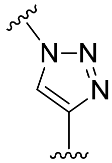	H	OCH_3	H	H	1,01	0,250 ± 0,010
22d		H	OCH_3	OCH_3	H	0,78	0,139 ± 0,003

Table 5.

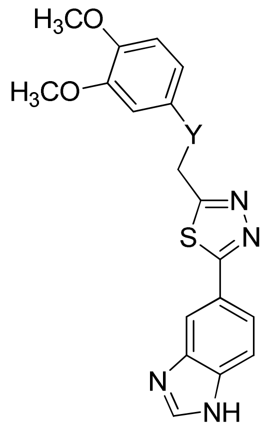

entry	Y	IC_{50} [μM]	K_i [μM]
8h	S	0.07	0.023 ± 0.001
8i	SO_2	0.52	0.080 ± 0.002

Table 6.

	No in Fig 2A	mutant	K_i (mutant)/K_i (wildtype) **8h**	**22b**	**benzmidazole**
Hydrophobic region	**1**	I303A	1.9	1.2	1.4
		I303N	2.3	1.2	1.8
		I303F	1.4	1.9	2.2
		I303V	0.6	0.7	1.2
	2	F325A	44.9	31.3	11.4
		F325N	18.9	28.7	6.7
		F325Y	32.3	31.3	5.6
	3	W329F	0.7	0.9	0.3
		W329Y	31.9	82.5	4.0
Hydrophillic region	**4**	W207F	1.6	1.4	0.8
		W207L	29.2	22.3	0.7
		W207Q	41.4	29.5	1.1
	5	H206A	0.8	0.9	1.0
		H206Q	1.2	1.1	0.9
	6	K144A	3.0	3.6	1.1
		K144M	4.0	3.1	1.1
		K144R	3.0	2.5	1.7

FIGURES

Figure 1. Alignment of the substrate H-Gln-Phe-Ala-NH_2, the inhibitors PBD150 (cpd. **53** in[17]) and the corresponding thioamide derivative (cpd. **81** in[17]). The Pharmacophore used for the virtual screening is represented by F1: encoding a metal-ligator, constraint to imidazole substructures; F3: encoding an H-bond donor; F2 and F5: encoding an H-bond acceptor; F4: encoding an aromatic center or a hydrophobic group.

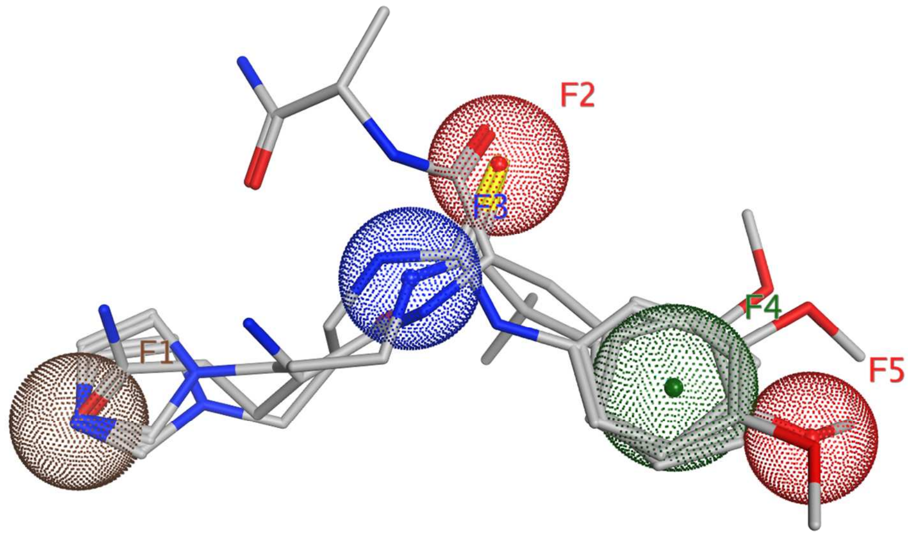

Figure 2. Potency of benzimidazole and the benzimidazole-1,3,4-oxadiazole derivatives, which were identified by pharmacophore search and confirmed as true hits. Compound **1a** was used as starting structure for a systematical SAR by a stepwise modification of the 5-membered heterocycle (green) the spacer group (yellow) and the hydrophobic/aromatic moiety (blue).

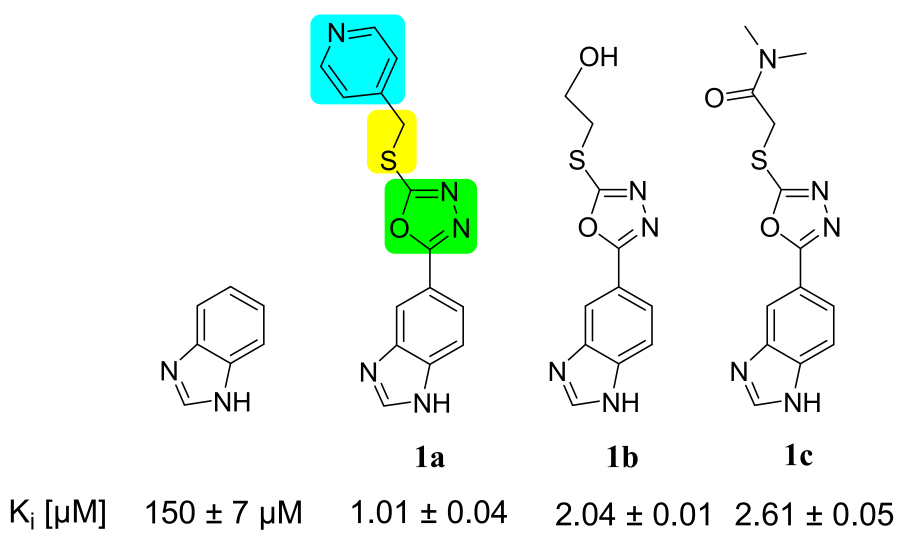

Figure 3. Tautomers of the compounds **8h** and **22b** leading to a Benzimidazole-6-yl derivative of **8h** (A) and **22b** (C) or Benzimidazole-5-yl derivative of **8h** (B) and **22b** (D) docked in the active site of human QC (pdb: 3si0, GOLDScore, 30 runs). The amino acids involved in the secondary binding of the inhibitors are annotated as in 3A with: 1: I303, 2: F325, 3: W329, 4: W207, 5: H206 and 6: K144. The transparency of the structures corresponds to the ranking regarding the score, the color (starting from yellow to blue) corresponds to the RMSD value with regard to the highest scored solution.

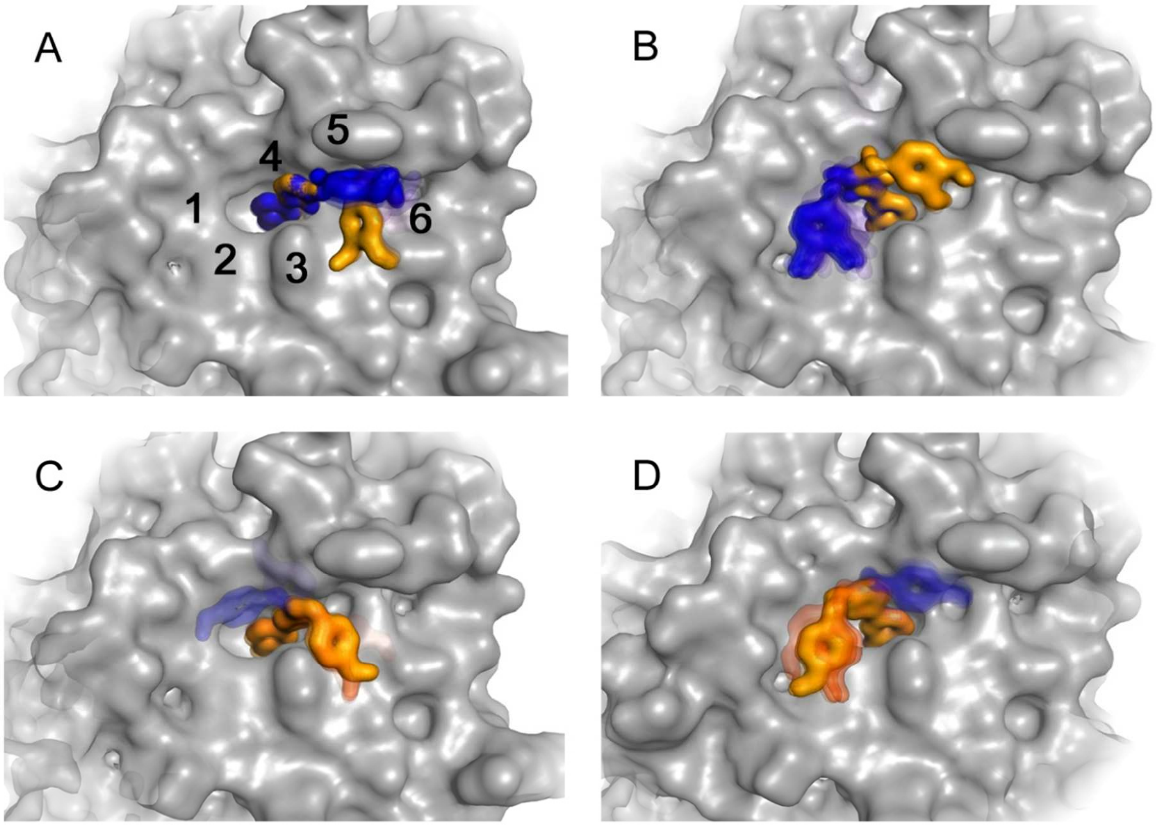

Figure 4. Influence of the mutation of different amino acids on the inhibition constants of **8h** and **22b** (pdb: 3si0; 1: I303, 2: F325, 3: W329, 4: W207, 5: H206 and 6: K144). The color code corresponds linear to the ratio $K_{i(mutant)}/K_{i(wildtype)}$, (Table 6), whereby the highest change for each mutation site was considered. (red: strong influence, green: no influence

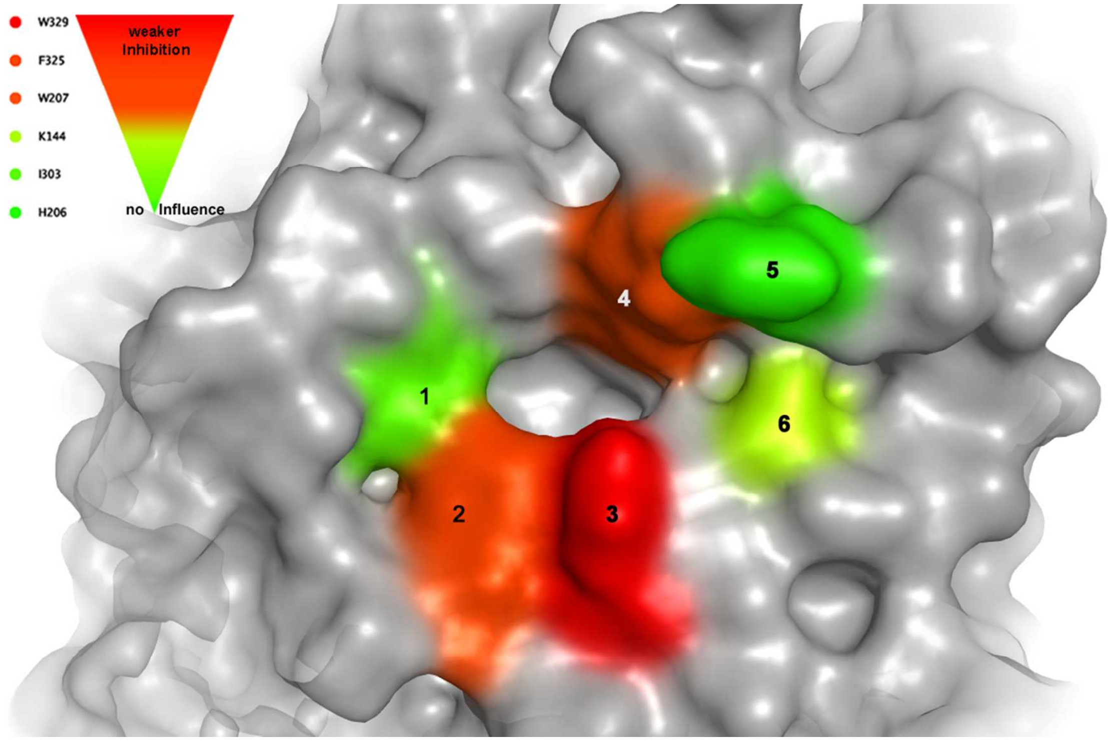

SCHEMES

Scheme 1[a].

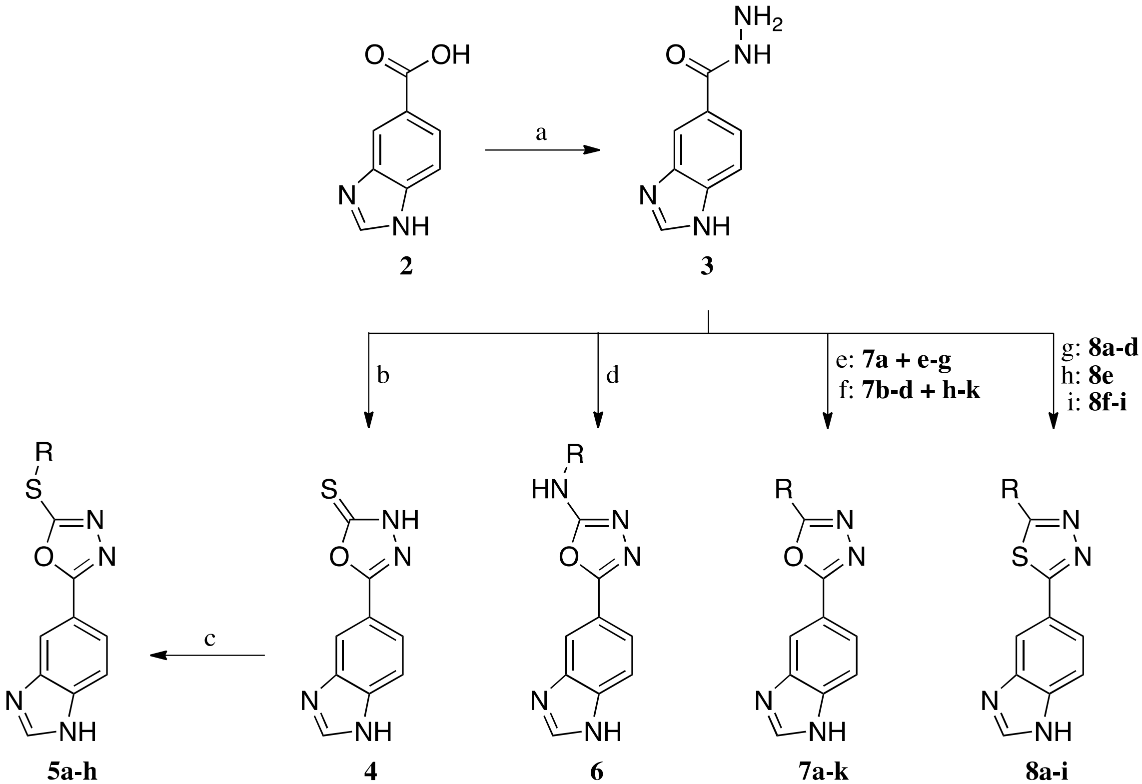

[a] Reagents and conditions: (a) H_2SO_4, EtOH, reflux, then N_2H_4*H_2O, EtOH, reflux; (b) CS_2, KOH, EtOH, reflux; (c) X-R, TEA, EtOH, reflux; (d) SCN-R, EtOH, reflux, then DCC, THF, reflux; (e) R-COCl, TEA, THF, rt then $POCl_3$, MeCN, reflux; (f) R-COOH, $POCl_3$, reflux; (g) R-COCl, TEA, rt, then Lawesson´s reagent, THF, reflux; (h) R-COOH, DCC, THF, rt-reflux, then Lawesson´s reagent, reflux; (i) R-COOH, Lawesson´s reagent, $POCl_3$, THF, reflux

Scheme 2[a].

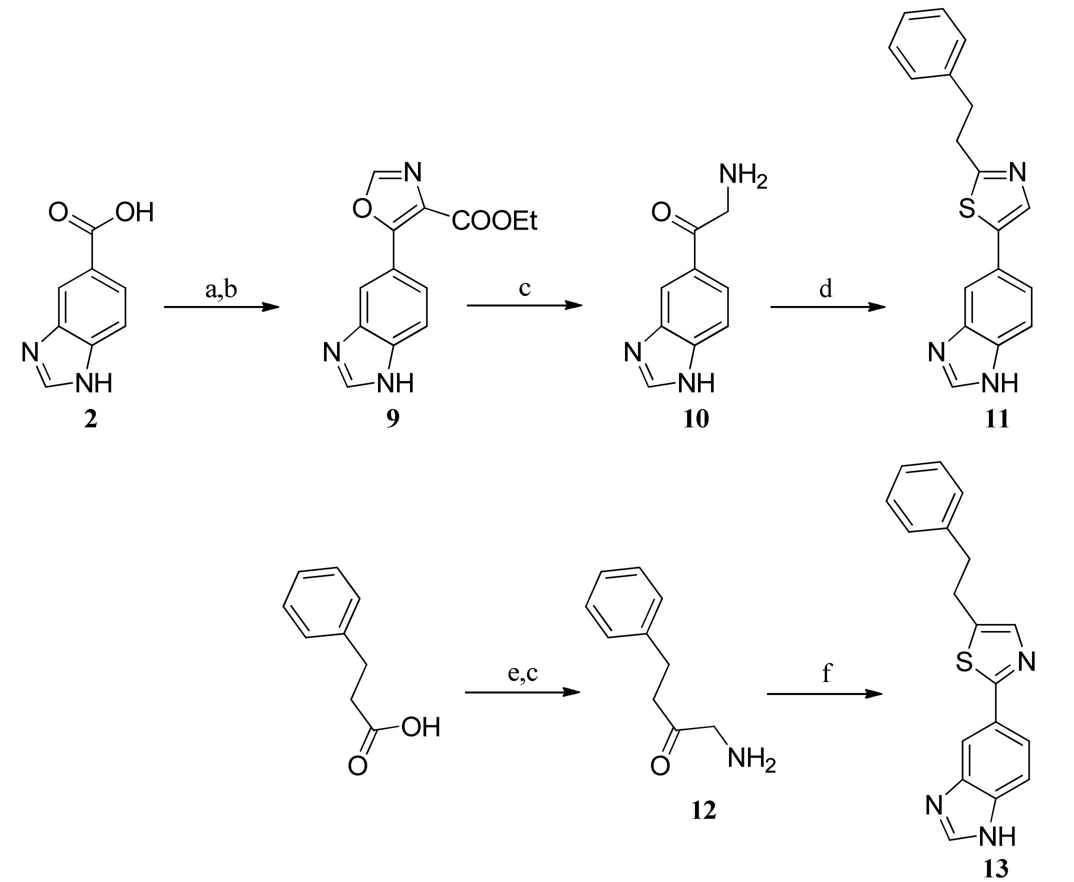

[a] Reagents and conditions: (a) $SOCl_2$, toluene, reflux; (b) $CNCH_2COOEt$, DBU, THF, rt; (c) $HCl_{(aq)}$, MeOH, reflux; (d) $Ph(CH_2)_2COOH$, Lawesson´s reagent, $POCl_3$, TEA, THF, reflux; (e) CDI, $CNCH_2COOEt$, DBU, THF, rt; (f) **2**, Lawesson´s reagent, $POCl_3$, TEA, THF, reflux

Scheme 3[a].

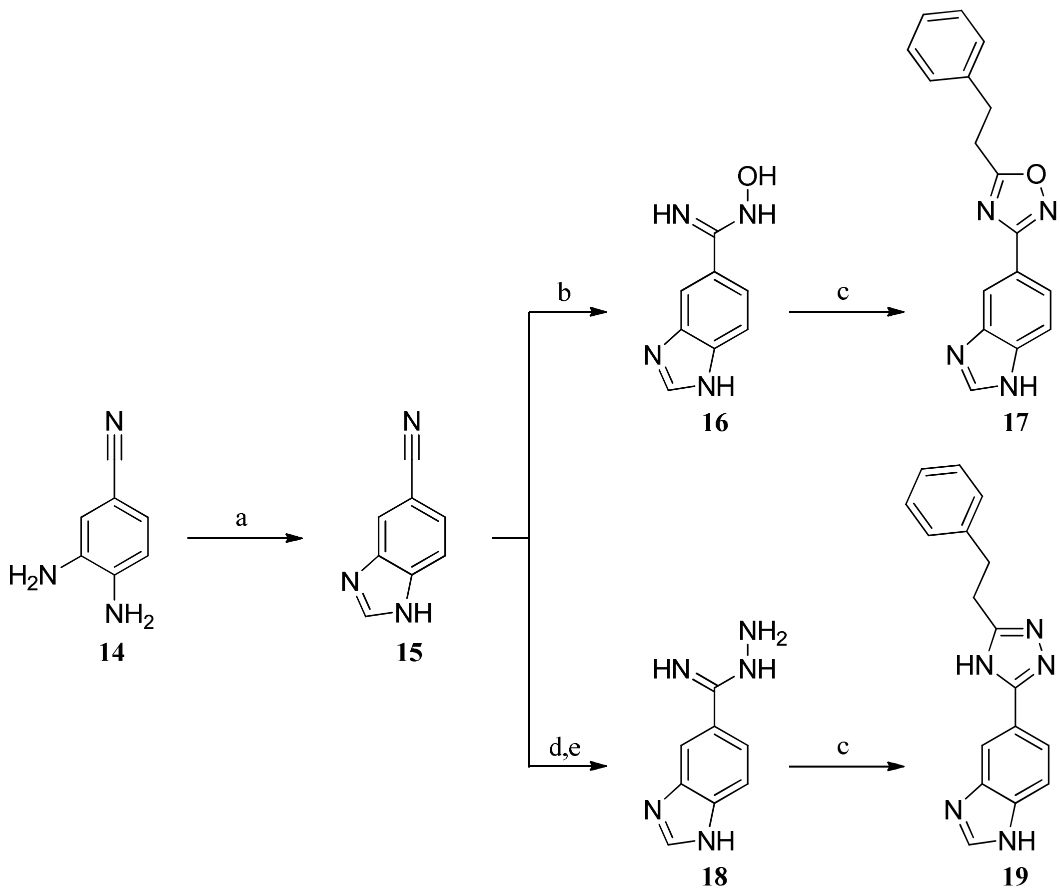

[a] Reagents and conditions: (a) HCOOH, 5 N HCl, reflux; (b) $H_2NOH*HCl$, K_2CO_3, EtOH, reflux; (c) $Ph(CH_2)_2COOH$, CDI, DMF, rt-110°C; (d) $HCl_{(g)}$, EtOH, 0°C-rt; (e) $N_2H_4*H_2O$, EtOH, rt

Scheme 4[a].

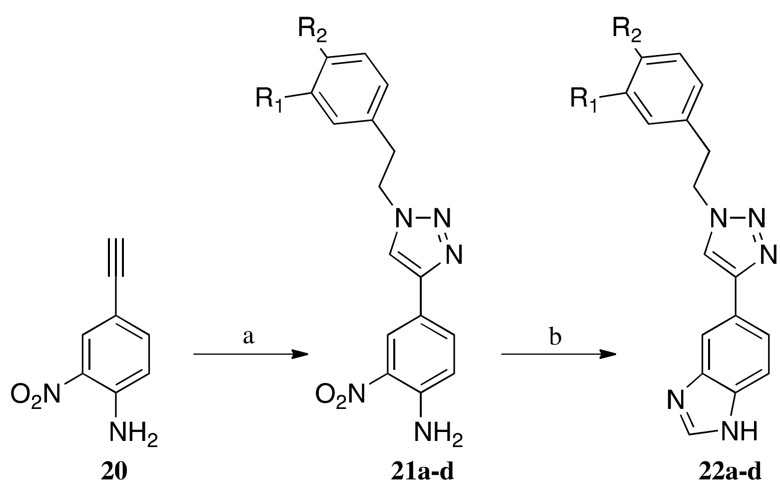

[a] Reagents and conditions: (a) $Ph(CH_2)_2Br$, NaN_3, DMSO, H_2O, $CuSO_4*5H_2O$, Na-ascorbate, rt; (b) HCOONa, HCOOH, Pd, $CH(OEt)_3$, 110°C

Table of Content Graphic:

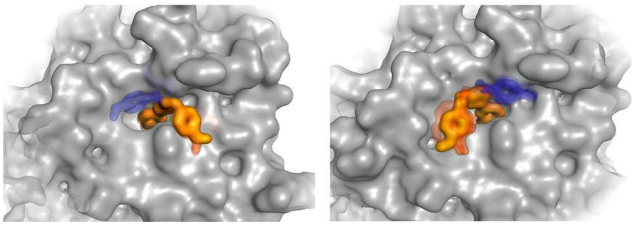

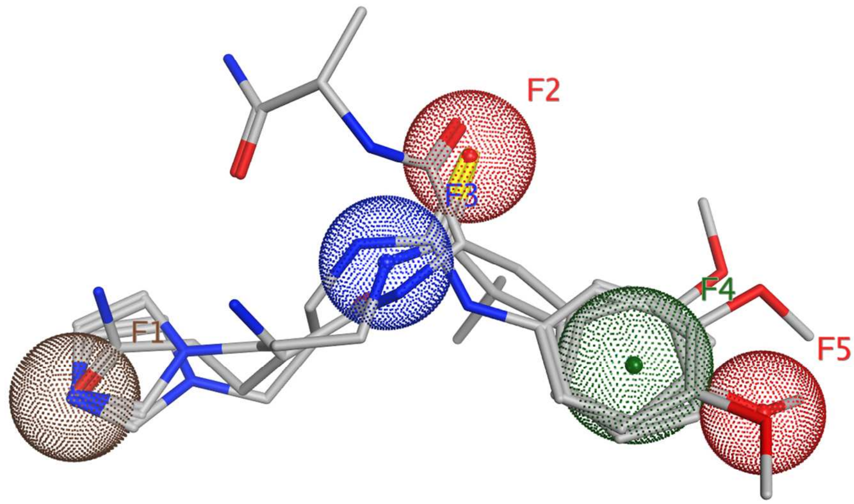

382x234mm (96 x 96 DPI)

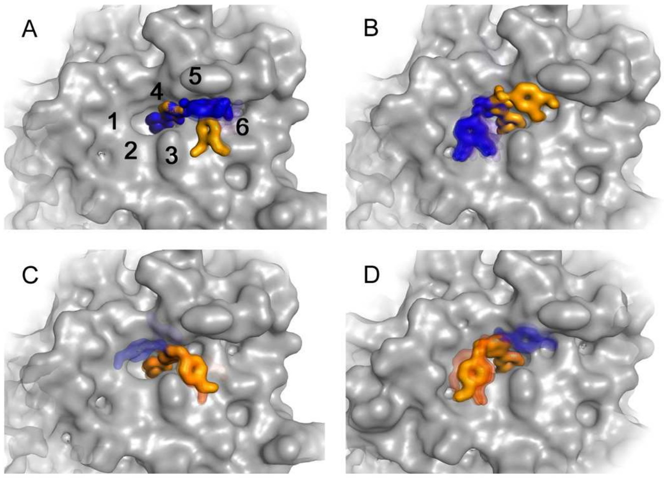

462x656mm (96 x 96 DPI)

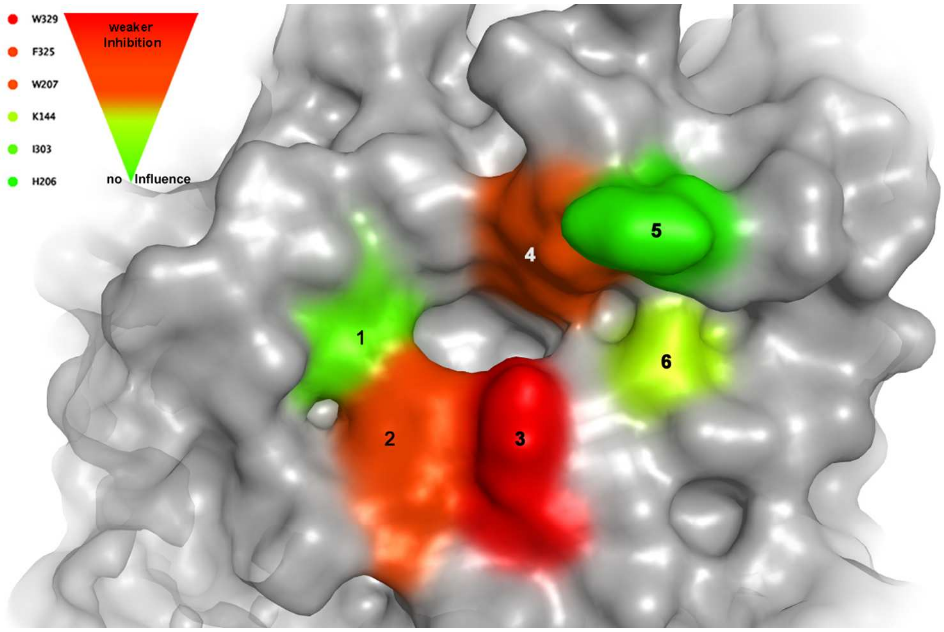

343x214mm (96 x 96 DPI)